COMPUTATIONAL MODELS CONSTRAINED BY VOLTAGE-CLAMP DATA FOR INVESTIGATING DENDRITIC CURRENTS

Alain Destexhe,[1,2] Diego Contreras,[2] Mircea Steriade,[2] Terrence Sejnowski[1,3] and John Huguenard[4]

[1] The Howard Hughes Medical Institute, The Salk Institute for Biological Studies, 10010 North Torrey Pines Road, La Jolla, California 92037

[2] Department of Physiology, Laval University School of Medicine, Québec, G1K 7P4, Canada

[3] Department of Biology, University of California San Diego

[4] Department of Neurology and Neurological Sciences, Stanford University Medical Center, Stanford, California 94305

ABSTRACT

We have investigated dendritic currents using a combination of experimental and modeling approaches. Voltage-clamp recordings were obtained in neurons with and without dendrites (intact vs. dissociated cells), and the recordings were compared to simulations that incorporated the corresponding dendritic morphology. This approach was applied to thalamic reticular cells to examine dendritic location of the low-threshold calcium current (I_{Ts}). The simulations matched the recordings only if I_{Ts} was located in distal dendrites with high density. Moreover, dendritic I_{Ts} was also necessary to reproduce the typical responses of these cells seen in intracellular recordings *in vivo*. This approach can be used to investigate other types of neurons with active dendritic currents.

INTRODUCTION

Thalamic reticular (RE) cells typically fire burst discharges, which play a central role in the genesis of various types of synchronized sleep oscillations and epileptic behavior (Steriade et al., 1993). A low-threshold Ca^{2+} current, I_{Ts}, underlies the production of these bursts (Bal and McCormick,1993; Huguenard and Prince 1992). As
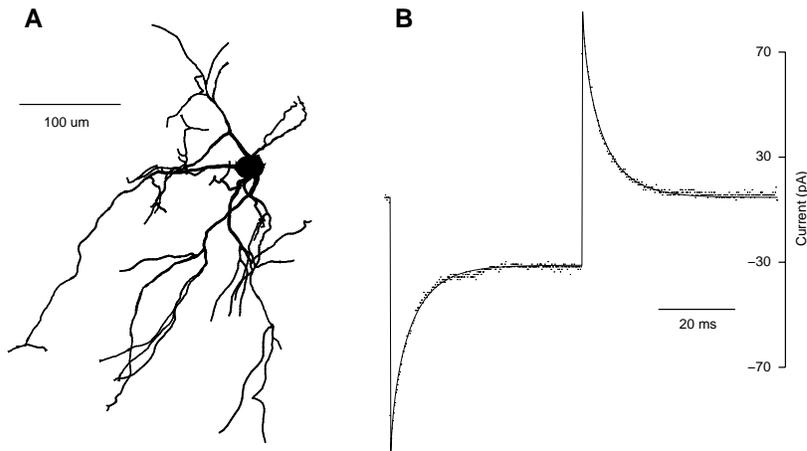
Figure 1.

Passive properties of thalamic reticular cells. A. Reconstructed RE cell from rat ventrobasal nuclei. B. Simplex fitting of the multicompartment model to voltage-clamp recordings from the same cell. Dots: current response from a -5 mV voltage-clamp step during 50 ms (holding potential of -80 mV; average of 8 traces). Continuous line: best simulation obtained after 450 iterations of the simplex procedure. The best parameters were: membrane capacitance of $1.01 \pm 0.01\ \mu F/cm^2$, axial resistivity of $260 \pm 30\ \Omega cm$, leak conductance of $0.05 \pm 0.0001\ mS/cm^2$ and reversal potential of $-82.844 \pm 0.002\ mV$ (modified from Destexhe et al., 1995).

suggested by Mulle et al. (1986), I_{Ts} may be localized in the dendrites. This may have important consequences for the synaptic control of the burst in RE cells (Destexhe et al., 1995).

In order to investigate the hypothesis of dendritic I_{Ts} in RE cells, we have combined computational models with electrophysiological recordings. Based on voltage-clamp recordings of RE cells with and without dendrites, and morphologically accurate models of these cells, we demonstrate that dendritic I_{Ts} can account for all voltage-clamp and current-clamp data.

METHODS

Recordings from dissociated cells and intact cells were compared to computer simulations to find the most likely distribution of calcium channels consistent with the available data (details of the procedures are given in Destexhe et al., 1995).

A cell from the ventrobasal sector of the RE nucleus of the rat was recorded and stained with biocytin (Huguenard and Prince, 1992). The morphology of the cell was then reconstructed using a three-dimensional tracing system with an accuracy of 0.1 μm (Eutectic Electronics) (Fig. 1A). This morphology was incorporated into NEURON to simulate the precise cable geometry of the recorded cell. Models with either 80 or 200 compartments were used.

A procedure based on a simplex algorithm was used to fit simulations directly to experimental data to find optimal values for parameters. At each iteration of the simplex algorithm, the model was run and the least square error was estimated between the simulated trace and the recording of the cell. The procedure was repeated until the model converged to a stable set of passive parameters from different initial conditions (Fig. 1B). The parameters obtained were in agreement with those determined in other types of cells (see e.g. Major et al., 1994; Rapp et al., 1994).

Voltage-dependent conductances were modeled using Hodgkin and Huxley (1952)

type of kinetic model. The Na^+ and K^+ currents responsible for fast action potentials were inserted in the soma. The kinetics of activation and inactivation of I_{Ts} in RE cells were based on voltage-clamp measurements (Destexhe et al., 1994). The densities of I_{Ts} were assumed to be different in the soma and in the dendrites.

Voltage-clamp recordings in acutely dissociated RE cells were used to characterize the kinetics of the low-threshold calcium current, I_{Ts} (Huguenard and Prince, 1992). In this preparation, the soma was present with only short dendritic appendages; the distal dendrites were removed. The voltage-clamp error was insignificant in these cells, as confirmed by simulations of dissociated cells (Destexhe et al., 1995). We used these kinetic data as the basis for quantifying the activation and inactivation of I_{Ts} channels.

Results

The simulations were first matched to voltage-clamp recordings in acutely dissociated RE cells, which lacked most of the dendritic arborizations. The amplitude of the current was adjusted to the experimental data (Fig. 2A,C) using a model with truncated dendrites. I_{Ts} was only included in the soma and the density of channels was adjusted to match the amplitude of the currents in Fig. 2A. In the intact cell, we were unable to obtain bursting behavior in current-clamp using the same distribution of I_{Ts} (Fig. 2D). About ten times higher densities of somatic I_{Ts} were needed to produce bursting activity (not shown), but the current amplitudes were then inconsistent with recordings on dissociated cells.

In intact RE cells, the peak amplitude of I_{Ts} was much larger than in dissociated cells (Destexhe et al., 1995), indicating that the T-current might be located in the dendrites. Thus, for these simulations, somatic I_{Ts} was deduced from recordings in dissociated cells, but a much higher density of dendritic I_{Ts} was necessary to obtain robust burst discharges (Fig. 2E).

Several observations further support a dendritic location for I_{Ts}. First, burst firing required large hyperpolarizing current injection; the burst had a slow rise and an *accelerando-decelerando* pattern of spikes (Fig. 2E). These patterns are typical features of RE cells (Contreras et al., 1993; Domich et al., 1986) and could not be obtained in simulated RE cells with only somatic I_{Ts}. Second, presumed dendritic recordings of RE cells showed striking similarities with the traces obtained in the model (see Destexhe et al., 1995). Third, voltage-clamp recordings in intact cells gave rise to slower time constants of I_{Ts} due to poor space clamp. The same features were observed in the model with dendritic I_{Ts}. Fourth, dendritic I_{Ts} replicated specific *in vivo* firing patterns of RE cells. In this case, sustained synaptic currents in the dendrites could simulate the properties of RE cells as seen from *in vivo* recordings, only if the major portion of I_{Ts} was dendritic (see Destexhe et al., 1995).

Finally, we applied a procedure for simplifying the dendritic morphology based on the conservation of the axial resistance (see Bush and Sejnowski, 1993). We showed that a three compartment model of the RE cell had equivalent electrophysiological behavior if T-channels had a high density in the distal dendrites (Fig. 3). This suggests that the typical electrophysiological behavior of RE cells is independent of the precise morphological details, provided the dendrites contain high densities of I_{Ts}.
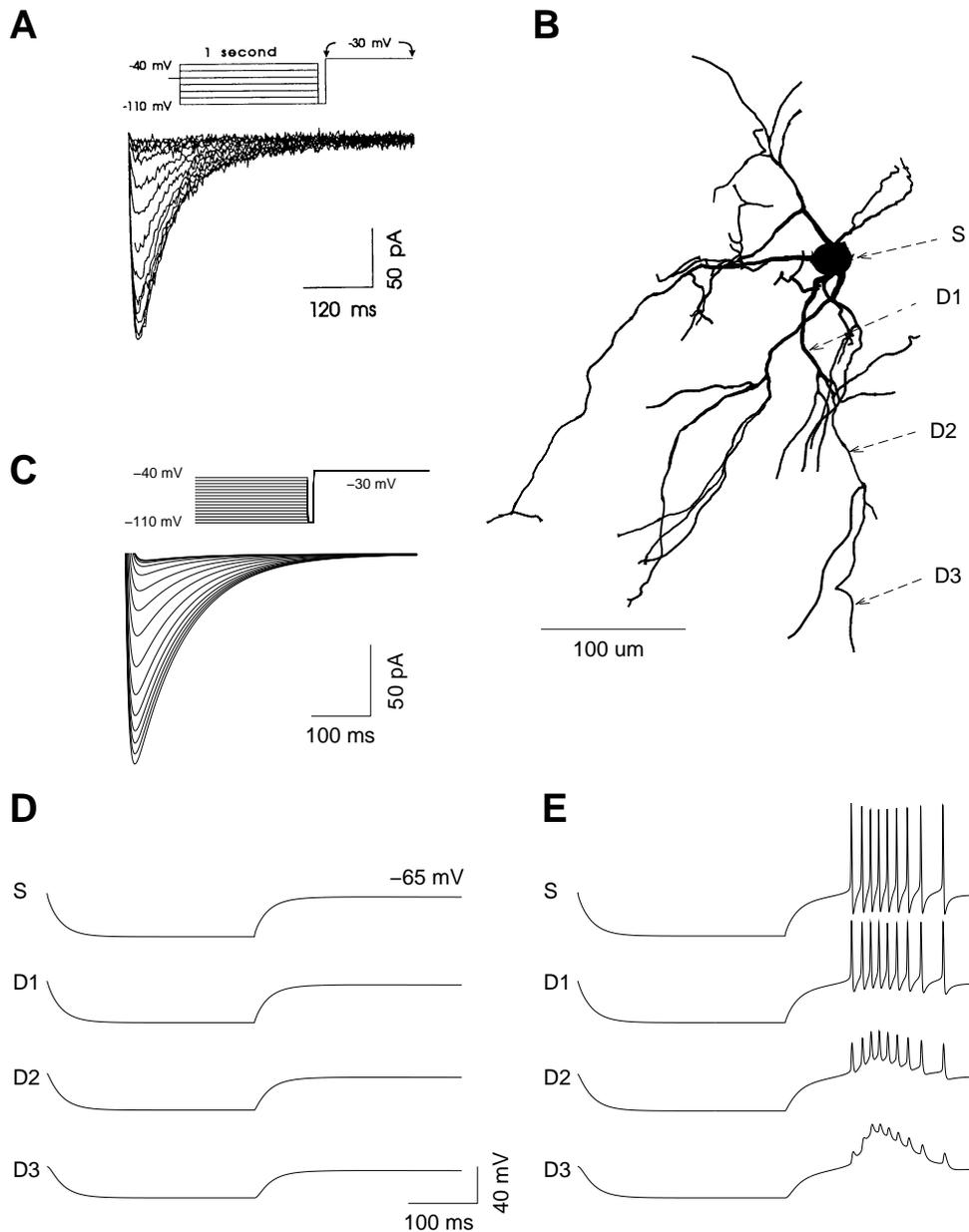
Figure 2.

Multicompartmental model of low-threshold calcium bursts in a rat thalamic reticular (RE) cell. A. Inactivation protocol of the low threshold Ca^{2+} current I_{Ts} on an acutely dissociated rat RE cell ($24\,^{\circ}C$; see Huguenard and Prince, 1992). B. Thalamic RE cell reconstructed from the same preparation. S, D1, D2 and D3 indicates dendritic locations depicted below. C. Simulations of the inactivation protocols described in A at $24\,^{\circ}C$, using the morphology shown in B with truncated dendrites. D. Current-clamp simulation with the same parameters as in C, but using the full morphology of the cell (B) at $36\,^{\circ}C$. E. Low-threshold burst discharge obtained by performing the same simulation as in D, but using high densities of I_{Ts} in the dendrites (modified from Destexhe et al., 1995).
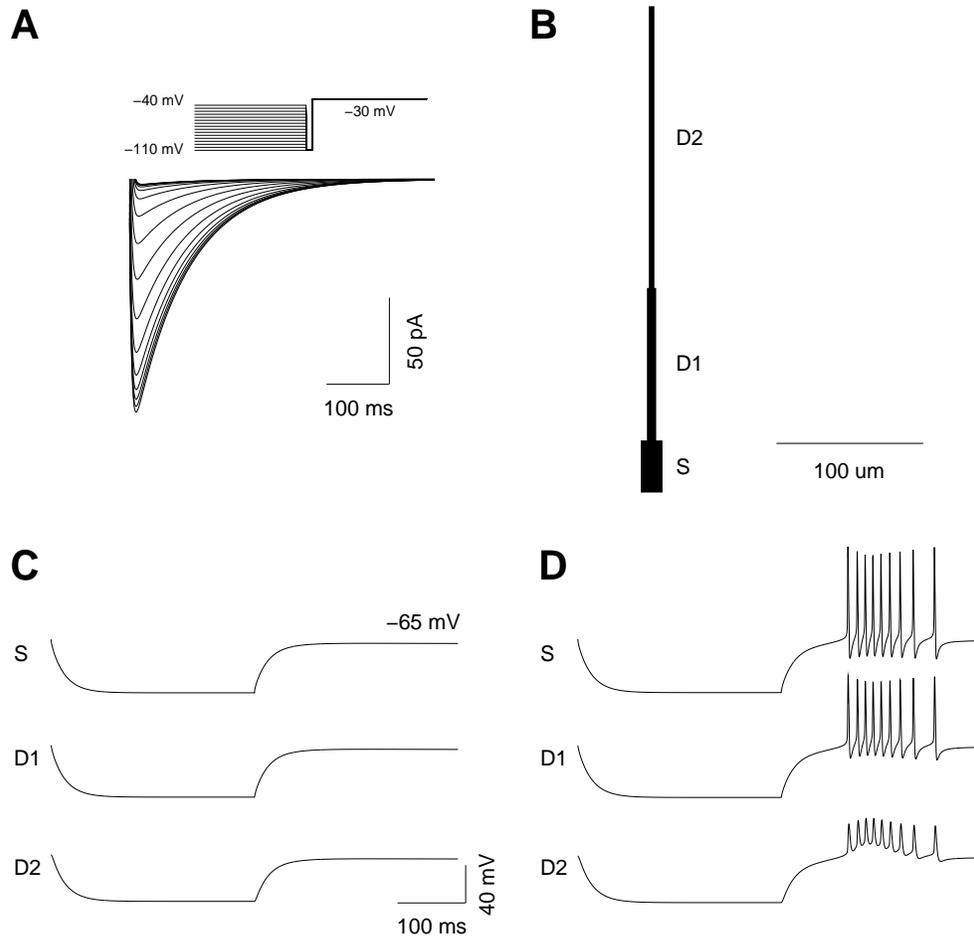
Figure 3.

Reduced model of low-threshold bursts in thalamic reticular cells. A. Simulated inactivation protocol of the low threshold Ca^{2+} current I_{Ts} (same description as Fig. 2A,C), using a three-compartment RE cell shown in B. B. Simplified dendritic morphology obtained by applying a reduction method based on the conservation of the axial resistance (Bush and Sejnowski, 1993). Starting from the morphology of the cell shown in Fig. 2B, the simplification procedure led to three compartments: the soma (S) as well as proximal (D1) and distal (D2) dendritic compartments. C. Current-clamp simulation using the same parameters as in A, with I_{Ts} located in the soma only. D. Same simulation as in C, but with a high density of I_{Ts} in the distal dendritic compartment. This model was about 25 times faster to simulate than the detailed morphological model in Fig. 2 (modified from Destexhe et al., 1995).

Summary and Conclusions

In conclusion, by matching computational models to voltage-clamp recordings of both intact and dissociated cells, we were able to put constraints on active currents in the dendrites. This method provided strong support for the hypothesis that dendritic I_{Ts} currents have an essential role in generating the bursting properties of RE cells observed in vivo. The same procedure could be applied to study bursting neurons in other regions of the brain.

Acknowledgments

REFERENCES

1. Steriade, M., McCormick, D.A. and Sejnowski., T.J. 1993 Thalamocortical oscillations in the sleeping and aroused brain. *Science* **262**: 679-685.
2. Bal, T. and McCormick, D.A. 1993 Mechanisms of oscillatory activity in guinea-pig nucleus reticularis thalami *in vitro*: a mammalian pacemaker. *J. Physiol.*, **468**: 669-691.
3. Huguenard, J.R. and Prince, D.A. 1992 A novel T-type current underlies prolonged calcium-dependent burst firing in GABAergic neurons of rat thalamic reticular nucleus. *J. Neurosci.* **12**: 3804-3817.
4. Mulle, C., Madariaga, A. and Deschênes, M. 1986 Morphology and electrophysiological properties of reticularis thalami neurons in cat: in vivo study of a thalamic pacemaker. *J. Neurosci.* **6**: 2134-2145.
5. Destexhe, A., Contreras, D., Steriade, M., Sejnowski, T.J., and Huguenard, J.R. 1995. In vivo, in vitro and computational analysis of dendritic calcium currents in thalamic reticular neurons. *J. Neurosci.*, in press.
6. Major, G., Larkmann, A.U., Jonas, P., Sakmann, B. and Jack, J.J.B. 1994 Detailed passive cable models of whole-cell recorded CA3 pyramidal neurons in rat hippocampal slices. *J. Neurosci.* **14**: 4613-4638.
7. Rapp, M., Segev, I. and Yarom, Y. 1994 Physiology, morphology and detailed passive models of guinea-pig cerebellar Purkinje cells. *J. Physiol.* **474**: 101-118.
8. Hodgkin, A.L. and Huxley, A.F. 1952 A quantitative description of membrane current and its application to conduction and excitation in nerve. *J. Physiol.* **117**: 500-544.
9. Destexhe, A., Contreras, D., Sejnowski, T.J. and Steriade, M. 1994 A model of spindle rhythmicity in the isolated thalamic reticular nucleus. *J. Neurophysiol.* **72**: 803-818.
10. Domich, L., Oakson, G. and Steriade, M. 1986 Thalamic burst patterns in the naturally sleeping cat: a comparison between cortically projecting and reticularis neurones. *J. Physiol.* **379**: 429-449.
11. Contreras, D., Curró Dossi, R. and Steriade, M. 1993 Electrophysiological properties of cat reticular thalamic neurones *in vivo*. *J. Physiol.* **470**: 273-294.
12. Bush, P.C. and Sejnowski T.J. 1993 Reduced compartmental models of neocortical pyramidal cells. *J. Neurosci. Methods* **46**: 159-166.